

Radiative feedback from protoplanets in self-gravitating protoplanetary discs

Sergei Nayakshin¹ and Seung-Hoon Cha^{1,2}

¹ *Department of Physics & Astronomy, University of Leicester, Leicester, LE1 7RH, UK*

² *Department of Physics & Astronomy, Texas A&M University-Commerce, P.O. Box 3011, Commerce, Texas, 75429, USA*

Received

ABSTRACT

It is well known that massive protoplanetary discs are gravitationally unstable beyond tens of AU from their parent star. The eventual fate of the self-gravitating gas clumps born in the disc is currently not understood, although the range of uncertainty is well known. If clumps migrate inward rapidly, they are tidally disrupted, which may leave behind giant or terrestrial like planets. On the other hand, if clumps migrate less rapidly, they tend to accrete gas, becoming proto brown dwarfs or low mass companions to the parent star.

Here we argue that radiative feedback of contracting clumps (protoplanets) on their discs is an important effect that has been overlooked in previous calculations. We show analytically that temperature in clump’s vicinity may be high enough to support a quasi-static atmosphere if the clump mass is below a critical value, $M_{\text{cr}} \sim 6$ Jupiter masses (M_J). This may arrest further gas accretion onto the clump and thus promote formation of planets rather than low mass companions.

We use numerical simulations to evaluate these analytical conclusions by studying migration and accretion of gas clumps as a function of their initial mass, M_i . Simulations neglecting the radiative preheating effect show that gas clumps with mass less than $\sim 2M_J$ migrate inward rapidly; more massive clumps result in low mass companions. In contrast, simulations that include radiative preheating from the clump show that clumps as massive as $8M_J$ migrate inward rapidly and end up tidally disrupted in the inner disc. We conclude that, with other parameters being equal, previous simulations neglecting radiative feedback from self-gravitating clumps over-estimated the population of brown dwarfs and low mass stellar companions and under-estimated the population of planets.

1 INTRODUCTION

Massive (e.g., $> 0.1M_{\odot}$) protoplanetary discs are expected to cool rapidly enough to fragment beyond tens to a hundred AU, depending on parameters of the problem (Gammie 2001; Mayer et al. 2004; Rice et al. 2005; Rafikov 2005; Durisen et al. 2007; Stamatellos & Whitworth 2008; Meru & Bate 2011). The exact fate of these clumps is however not well known because of the physical and numerical uncertainties of the calculations (e.g., Stamatellos & Whitworth 2009b), and because of a huge parameter space (e.g., disc opacity, dust physics more generally, angular momentum of the incoming material, mass deposition rate into the disc, external illumination, etc.).

A subset of authors, e.g., Vorobyov & Basu (2006, 2010), Boley et al. (2010), Cha & Nayakshin (2011), Machida et al. (2011) find repeated clump formation followed by inward clump migration and tidal destruction in the inner disc. This process inspired a new “Tidal Downsizing” scenario for planet formation (Boley et al. 2010; Nayakshin 2010a) that can *potentially* explain formation of

all types of planets, although much work is to be done to rigorously test and develop this model further.

Two further publications, Michael et al. (2011) and Baruteau et al. (2011) presented simulations of marginally stable self-gravitating discs with a single planet inserted into the disc and treated as a point mass (which disallows further gas accretion onto the planet), and found that the planets did migrate inward on the time scale of just a few orbits.

On the other hand, a number of other authors did not find such a strong clump migration. For example, disc simulations by Stamatellos & Whitworth (2008, 2009a) show formation of many more brown dwarfs than planet-mass objects, and these do not appear to migrate inward in the discs that much. Note that earlier β -prescription cooling simulations, such as Rice et al. (2005), cannot be useful here because these simulations typically stall due to increasingly small timesteps needed to integrate dense clump evolution when one or more clumps are formed. Finally, a recent study by Zhu et al. (2012) find that the outcome of clump formation is not a single outcome process, with 6 of their 13 clumps migrating in and crossing the inner boundary, 4 migrating and being tidally destroyed before reaching the in-

ner boundary, and 3 becoming brown dwarfs and stalling their migration in the outer disc as they open deep gaps. Zhu et al. (2012) suggested that it is a competition between clump migration and accretion onto the clump that appears to decide which of these outcomes takes place.

In this paper we point out yet another physical complication than will have to be modelled robustly enough before the community arrives at a firm conclusion about the non-linear outcome of the gravitational disc instability. In particular, all of the gravitationally unstable disc simulations performed so far employed a prescription of some kind to approximate radiative transfer out of the disc. None of these looked into how the energy release within the gas clump (protoplanet) may affect the surrounding gas in the disc. To see that this “preheating” effect may be significant, consider the accretion luminosity of the *whole* protostellar disc at the unstable region, $R \sim 100$ AU:

$$L_{\text{disc}} \sim \frac{GM_* \dot{M}_*}{2R} \approx 10^{-3} L_{\odot} \frac{\dot{M}_*}{10^{-6} M_{\odot} \text{yr}^{-1}}, \quad (1)$$

where $M_* \approx 1 M_{\odot}$ is the mass of the protostar, and \dot{M}_* is the accretion rate in the disc.

Now protoplanetary clumps of a few to $10 M_J$ can be as bright as this or even brighter at birth (e.g., Nayakshin 2010b; Zhu et al. 2012). This luminosity is therefore bound to significantly heat up the gas near the clump’s location.

We present in §2 “radiative zero atmosphere” analytical arguments, familiar from the physically similar situation encountered during the growth of giant planets in the CA scenario (Mizuno 1980; Stevenson 1982). These arguments show that the contraction luminosity of the young protoplanet supports a hot atmosphere around the protoplanet, preventing further accretion of gas onto it. Just as in CA theory, we show that there should exist a critical protoplanet mass, M_{cr} , above which the radiative atmosphere solution is unstable to self-gravity and should collapse onto the protoplanet. The implications of this argument are that previous numerical simulations that neglected radiative feedback from the protoplanets may have over-estimated the accretion rate of gas onto the clumps, thus over-produced low mass stellar companions and brown dwarfs, and under-produced lower mass objects – planets.

We run numerical simulations with and without protoplanetary feedback to investigate these ideas more quantitatively. We set up a disc in a marginally gravitationally stable regime and then insert a density enhancement of a specified total mass inside of a spiral arm. We confirm the Zhu et al. (2012) findings that the fragments stall when they accrete a significant amount of gas from the disc. Specifically, without protoplanetary feedback, only protoplanets with initial mass $M_p \lesssim 2M_J$ migrated inward faster than they accreted gas. These planets migrated inward sufficiently fast to be tidally disrupted. However protoplanets with masses M_p larger than that gained too much mass too quickly and stalled, becoming proto brown dwarfs or low mass stellar companions rather than planets.

Simulations which take the protoplanetary feedback into account via a prescription (see §3.2) show that gas accretion is indeed significantly slowed down, so that clumps with an initial mass of as much as $8M_J$ migrate rapidly and are tidally disrupted.

We conclude that the non-linear outcome of clump for-

mation in the outer self-gravitating disc strongly depends on the temperature structure near the protoplanet. Future work must include the preheating effects in order to obtain reliable results.

2 A QUASI-EQUILIBRIUM ATMOSPHERE AROUND THE GAS CLUMP

First of all, we make a note on terminology: it is not exactly clear when one should call a self-gravitating gas clump “a planet”. One may choose to consider Hydrogen molecules dissociation and formation of a very dense “second core” as a sign post of planet formation (e.g., Stamatellos & Whitworth 2009b). On the other hand, such a planet may accrete more mass from the disc, becoming a brown dwarf or even a low mass star, or, on the contrary, migrate very close to the parent star and be unbound by tides at separations of ~ 0.1 AU (Nayakshin 2011). This may leave just a solid core behind or nothing at all, if the “planet” was already too hot for dust sedimentation (Helled & Schubert 2008). In this paper we cannot trace all these possible outcomes, so we simply define a planet as any “obvious” dense self-gravitating gas condensation. Therefore, a “gas clump” and a “planet” are synonymous here.

Before we begin our numerical investigation, we appeal to the following parallel: accretion of the gaseous envelope on the top of a solid core immersed in a protoplanetary disc in the context of the CA model (e.g., Mizuno 1980). It is well known that at a given core luminosity, L_c , there exists a critical core mass, M_{cr} . Cores with mass less than M_{cr} are surrounded by a gaseous hydrostatic atmosphere. Atmospheres of cores with mass larger than M_c are too massive (comparable in mass to M_{cr}) for a hydrostatic solution to apply; they “collapse” onto the solid core. This sets off an accretion phase onto the solid core and eventually results in formation of a giant planet.

The situation we are concerned about is actually analogous to this classical result from the CA theory, except that the role of the dense core is played by the dense – mainly gaseous – protoplanet. The luminosity of the protoplanet here is not due to accretion of planetesimals but is rather due to contraction of the protoplanet.

We follow the analytical argument first presented by Stevenson (1982) and solve for the structure of a “radiative zero atmosphere” around a point mass planet of mass M_p and luminosity L_p . Since no energy is released in the atmosphere, the luminosity is

$$L_p = -\frac{16\pi r^2}{3} \frac{\sigma_B}{\kappa \rho} \frac{dT^4}{dr} = \text{const}, \quad (2)$$

where ρ and T are the gas density and temperature distance r away from the protoplanet’s centre. Further, writing the standard equation of hydrostatic balance for the atmosphere, we find (see, e.g., Armitage 2010) for the temperature, $T(r)$, and density, $\rho(r)$, profiles in the atmosphere:

$$T(r) = T_{\text{rad}} = \frac{GM_p \mu m_p}{4k_B r}, \quad (3)$$

$$\rho(r) = \frac{64\pi\sigma_B}{3\kappa R L_p} T^4(r) r \propto \frac{1}{r^3}, \quad (4)$$

where κ_R is the Rosseland mean opacity and $\mu \approx 2.45$ is the mean molecular weight.

This solution is approximately valid for $r \geq r_p$, where r_p is the planet's radius, and as long as the envelope's mass, $M_{\text{env}} = \int_{r_p}^{r_H} dr 4\pi r^2 \rho(r)$, is negligibly small compared with M_p . Here $r_H = a(M_p/3M_*)^{1/3}$ is the Hill's radius of the planet located a distance a from the parent star of mass M_* . The envelope's mass is given by

$$M_{\text{env}} = \frac{\pi^2 \sigma_B}{3\kappa_R L_p} \left(\frac{GM_p \mu m_p}{k_B} \right)^4 \ln \left(\frac{r_H}{r_p} \right). \quad (5)$$

We observe from equation 5 that at a constant L_p the envelope's mass is increasing as $M_{\text{env}} \propto M_p^4$; therefore, there will be a maximum M_p at which the envelope's mass becomes comparable to M_p . As in CA, the envelope in this case should contract rapidly due to its own self-gravity. Thus, the condition $M_{\text{env}} \approx M_p$ marks the critical planet's mass above which a rapid accretion of additional mass from the surrounding disc sets in.

Protoplanets are very bright at formation, up to $L_p \sim 10^{-2} L_\odot$ (Nayakshin 2010b), and are extended, thus not much smaller than r_H . Scaling the result to this fiducial value of L_p , and setting $\ln(r_H/r_p) \sim 1$, we obtain

$$M_{\text{crit}} \approx 6M_J \left(\frac{L_p}{0.01 L_\odot} \right)^{1/3} \left(\frac{\kappa_R}{0.1} \right)^{1/3} \quad (6)$$

This derivation of the critical mass is rather approximate, as many additional effects are important in real protoplanetary discs. For example, (a) the protoplanet's luminosity decreases with time, (b) it is also a function of the planet's mass itself; (c) the envelope's contraction luminosity may not be neglected if its contraction becomes sufficiently fast; (d) the tidal field of the star contributes at $r \lesssim r_H$ to loosen the envelope; (e) the envelope eventually may become optically thin, so that the temperature profile at large r would be shallower; (f) the envelope's temperature and density cannot fall below those of the surrounding disc at large radii. Some of these effects act to increase M_c , others to decrease its value. We could try to include some of these effects in our analytical model here, but unfortunately this is not worthwhile: the 1D approach cannot be very accurate in the given situation as the flow of gas around the planet is distinctly a 3D pattern. Therefore, we move on to 3D simulations in the next sections. In the next section we describe a procedure with which we hope to capture the essence of the radiative preheating effect in our planet-disc simulations.

3 NUMERICAL APPROACH

3.1 Overall method

Our numerical approach follows that described in Cha & Nayakshin (2011) except for a different cooling function and initial conditions. Cha & Nayakshin (2011) used a cooling time prescription that was a function of gas density only, smoothly joining the low and the high gas density regimes. This treatment is best for the gas within the protoplanet itself, as it follows the semi-analytic model of molecular clump cooling due to dust opacity by Nayakshin (2010b). The relatively low density regime, as appropriate for the ambient disc rather than the clump, was modelled with a

simple assumption of a constant cooling time of 100 years. This simple approach yielded the appropriate radial range for disc fragmentation as obtained both analytically and numerically, e.g., $R \sim 70$ AU (e.g., Rafikov 2005; Boley et al. 2010).

Here our focus is the material of the disc close to the planet's location. Therefore we employ a more detailed although still approximate approach to radiative cooling, following a number of authors (e.g., Johnson & Gammie 2003; Boley et al. 2010; Vorobyov & Basu 2010). We write the energy loss rate per unit time per unit volume as

$$\Lambda = (36\pi)^{1/3} \frac{\sigma_B}{s} (T^4 - T_{\text{irr}}^4) \frac{\tau}{\tau^2 + 1}, \quad (7)$$

where $T_{\text{irr}} = 10$ K is the background temperature set by external irradiation, τ is the optical depth estimate, given by $\tau = \kappa(T)\rho s$ (cf. Galvagni et al. 2012). The lengthscale s is given by $s = (\mathcal{M}/\rho)^{1/3}$, where $\mathcal{M} = 10M_J$, and varies from a few AU to tens of AU for the range of densities found in the simulation. The opacity law is $\kappa(T) = 0.01(T/10\text{K})$, as in the analytical model of Nayakshin (2010b).

As is well known, "first cores" hotter than $T \sim 2000$ K cannot exist, since hydrogen molecules start to dissociate (Larson 1969). This process presents a very large internal energy sink, so that the clump behaves nearly isothermally at $T \gtrsim 2000$ K, which invariably leads to the second collapse during which the first core contract to much higher densities and becomes the "second core". To mimic this behaviour, we impose a maximum temperature for our gas, $T_{\text{max}} = 2500$ K, and introduce a sink particle inside the clump when the density of the clump exceeds $\rho_{\text{sink}} = 10^{-8} \text{ g cm}^{-3}$. The sink radius is 5 AU.

We do not include the dust component in the present numerical simulations, in contrast to Cha & Nayakshin (2011).

3.2 Radiative preheating of the disc

In our exploratory model we make a number of simplifying assumptions and approximations. Firstly, the planet's luminosity is given by

$$L_p(M_p) = 1.5 \times 10^{31} \text{ erg s}^{-1} \left(\frac{M_p}{10M_J} \right)^{5/3}. \quad (8)$$

This is based on the analytical model of Nayakshin (2010b) at $t = 0$. We note that the contraction luminosity of a planet actually decreases with time, but in our simulations the planet's mass may be evolving (usually increasing), and therefore it is not clear what to take for $t = 0$. This should not lead to significant uncertainties in the results, however, because the planet's luminosity at a constant M_p decreases only by a factor of a few over the duration of our simulations.

With this in mind, we calculate the radiative gas temperature, T_{rad} , a distance r away from the centre of the clump assuming the radiative equilibrium for the gas around the clump. We view T_{rad} as the *minimum* gas temperature at this location, arguing that any additional heating processes not taken into account in this analytical treatment would result in a higher temperature. For example, local contraction luminosity (e.g., "PdV" work due to planet's envelope contraction) and shocks could increase gas temperature above T_{rad} . Operationally, we calculate the gas temperature, T , at

locations of SPH particles, solving the energy equation that includes compressional heating and shocks minus the cooling rate given by equation 7. If T falls below T_{rad} we set $T = T_{\text{rad}}$.

When calculating T_{rad} , we consider three different regions in order of their distance r from the clump’s centre: (1) inside the clump, $r \leq r_p$; (2) outside the clump but within one disc scaleheight, H , e.g., $r_p \leq r \leq H$; and finally, (3) $r > H$. As gas density in the disc is largest in the disc midplane, decreasing in directions perpendicular to it, most of the clump “atmosphere” mass is located near the midplane of the disc. Therefore we now search for an approximate temperature structure near the clump only along the midplane of the disc.

The energy balance in the disc geometry dictates that the radiative flux out of the optically thick disc in the direction perpendicular to the midplane, $F_{\perp} \approx \sigma_B T^4 / \tau$ is equal to the column-integrated heating rate (e.g., Shakura & Sunyaev 1973), where τ is the optical depth estimated as described in section §3.1. Since we are only setting here the minimum temperature of the gas due to the radiative preheating from the protoplanet, our radiative preheating energy balance requires that $F_{\perp} \approx F_r$, where F_r is the radiative flux from the planet. In the region $r_p < r < H$, $F_r \approx L_p / 4\pi r^2$, which yields

$$T_{\text{rad}} \approx \left[\frac{L_p(1+\tau)}{4\pi r^2 \sigma_B} \right]^{1/4}, \quad (9)$$

where we replaced τ with $(1+\tau)$ to account for the optically thin limit in case $\tau \lesssim 1$. While equation 9 appear to be different from the radiative zero solution (equation 3) for a spherical geometry, we shall see in section ?? that the two profiles are actually quite similar in practice.

At distances $r \gtrsim H$ from the planet we need to take additional consideration of the “leakage” of the radiative flux from the disc in the vertical direction. An approximate solution formally correct in the limit $H \ll R$ and a constant disc density (as a function of r) yields that the radiation flux density at $r \gg H$ is reduced by the factor $\sim \exp[-r/H]$. Thus we write for $r > H$

$$T_{\text{rad}} \approx \left[\frac{L_p(1+\tau)}{4\pi r^2 \sigma_B} \exp\left(-\frac{r}{H} + 1\right) \right]^{1/4}, \quad (10)$$

which then makes T_{rad} continuous at $r = H$.

Finally, inside the planet itself, L_p cannot be considered constant: the radiative flux is exactly zero at $r = 0$ as $dT/dr = 0$ at the centre of the clump. Therefore we set $L_p(r) = (r/r_p)^2 L_p$ for $r \leq r_p$ and then use this value of L_p in equation 9. In practice this latter prescription makes the radiative “preheating” within the planet completely negligible, as of course should be the case.

We also set $r_p = 5$ AU for simplicity when we calculate the clump mass “on the fly” during simulations. Numerically, we find the densest part of the protoplanet, define that location as the planet’s centre, and then calculate the current mass of the protoplanet, $M_p(t)$, as the mass within the fixed radius r_p . We found that our planets – that is dense gas clumps resulting from gravitational collapse of the initial perturbations introduced at $t = 0$ – are always smaller than a few to 5 AU, and therefore we fixed $r_p = 5$ AU. This approach is conservative: if anything, it underestimates the im-

portance of preheating when the planet contracts to smaller sizes. Finally, we also fix $H = 10$ AU when we calculate T_{rad} in equation 10.

3.3 Initial conditions and simulations performed

The initial mass of the star is set to $M_* = 0.7 M_{\odot}$ in all the simulations. The star is allowed to grow by accretion of gas from the protoplanetary disc if the gas crosses the accretion radius of 10 AU.

We are interested in a marginally gravitationally *stable* protoplanetary disc that may self-regulate its mass by the episodic creation of gas clumps that migrate inward quickly (Vorobyov & Basu 2010). At the same time we would like to avoid non-linear clump-clump interactions (cf., e.g., Boley et al. 2010; Cha & Nayakshin 2011) as much as possible, concentrating on one clump at a time. Therefore, we first of all find a self-gravitating disc configuration that is on the verge of fragmenting. In particular, we set a grid of simulations with discs initially extending from 20 to 200 AU, with the radial profile $\Sigma_0(R) \propto 1/R$, and the initial disc masses, M_d , in the range from 0.2 to 0.4 M_{\odot} . The disc material is initially set on circular orbits around the protostar.

We then follow the disc evolution for ~ 10 orbits at the outer disc edge. We found that the disc with the initial mass of $M_d = 0.325 M_{\odot}$ does not fragment, although shows 2 strong spiral arms. We note that the spiral density waves in this rather high mass disc transfer angular momentum quickly, as expected (Lodato & Rice 2005), so that the disc becomes less unstable as time progresses. Therefore we are confident that the disc in this simulation would not fragment even if we continued the simulation for an infinitely long time. On the other hand, the disc with an initial mass of $M_d = 0.35 M_{\odot}$ fragmented on a number of clumps, with a complicated behaviour reminiscent of that found in Cha & Nayakshin (2011).

We thus select the disc with $M_d = 0.325$ at time $t \approx 10,000$ years as our starting initial condition. A density perturbation is then inserted in the disc in a very simple way, e.g., by increasing the gas density in a selected region by a factor of 4. In practice this is done by adding new SPH particles in the region. These new particles copy the density, temperature and velocity fields of the existing SPH particles in the region; the coordinates of the new SPH particles are shifted by a small distance, $h_s/5$, from their “parent” particles in random directions. Here h_s is the SPH smoothing length of the parent particle. Our results are essentially independent of the exact procedure in which the perturbation is inserted since we allow the region to contract and relax somewhat before radiative preheating is turned on (see below).

The location of the perturbation is set to be at the radial distance of 75 AU from the parent star (which is close to the radial location of the minimum in the Toomre’s Q -parameter) at the densest part of the spiral arms. The surface density of the initial disc with perturbation of mass $M_i = 4M_J$ is shown in Figure 1.

With this identical approach and numerical scheme we run a set of simulations with and without planet feedback on its surroundings and the initial perturbation mass varying between $0.5M_J$ and $16M_J$ in increments of factor of two.

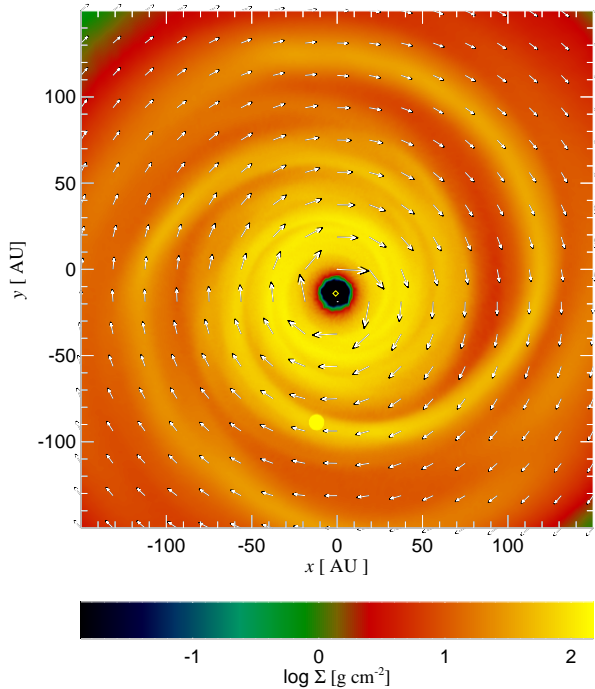


Figure 1. The surface density of the initial marginally stable self-gravitating disc at time $t = 0$, plus the initial perturbation (“protoplanet”) of mass $M_p = 4M_J$, located at $R = 75$ AU. The perturbation is inserted as described in §3.3. The vectors in the figure show the gas velocity field.

The corresponding runs are labelled MX or MXF, where X is the mass of the initial perturbation in Jupiter masses.

In the runs with feedback, the feedback is “turned on” after half a rotation. This measure is taken to allow the initial perturbation to actually contract gravitationally into a well defined self-bound clump before any feedback is produced.

4 OVERVIEW OF RESULTS

Figure 2 presents the planet-star separation, a , of the simulated planets versus their mass. The initial masses of the planets are $0.5M_J$, 1 , 2 , 4 , 8 , and $16M_J$ for the red, blue, green, violet, cyan and black curves, respectively. As explained at the end of section 3.2, to avoid ambiguities as to what is a planet, we measure the planet’s mass as that within a fixed radius of 5 AU for this figure. We find that at later times all the planets contract sufficiently to be within ~ 5 AU. For the lowest mass perturbations, this procedure slightly over-estimates the initial planetary mass somewhat, whereas for the highest mass perturbation the planetary mass is underestimated (which is why the initial masses of planets in the figure may appear slightly different from the values quoted above). However, this convention affects only the first \sim half a rotation of the planets around their parent stars in the simulations and has a very minor effect on the final results.

The end of the simulation here is defined either when the protoplanet is completely destroyed by tidal torques, or

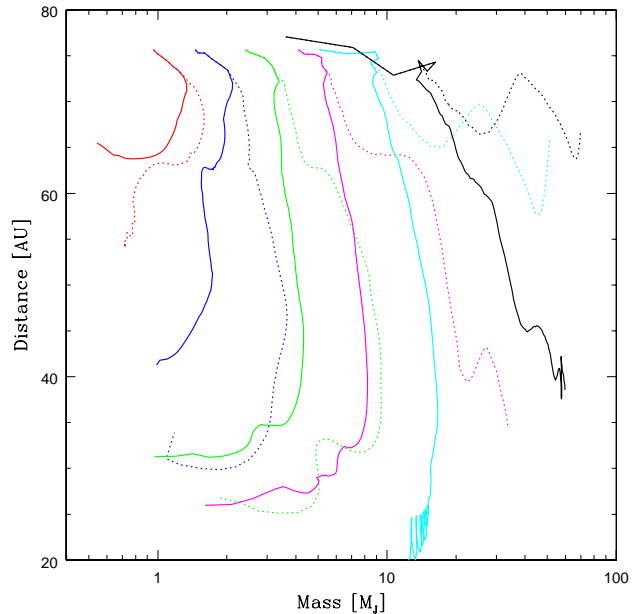


Figure 2. Protoplanet-star separation versus planet’s mass, M_p , for all of the simulations presented in this paper. The runs with feedback are shown with solid curves, whereas those without feedback are dotted. The protoplanet’s initial masses are $0.5M_J$ for the red curves, and increase by factor of two each time when moving to higher mass cases. See §4 for more detail.

gains a sufficient amount of mass to become the “second core” (Masunaga & Inutsuka 2000), which in these simulations is always of a brown dwarf mass.

In Figure 2, results for runs with feedback are shown by solid curves, whereas those without feedback are dotted. Same colours are used for runs with the same initial perturbation mass. A planet growing in mass at a constant separation would trace a horizontal track, while a planet migrating radially at a constant mass would be on a vertical line.

Initially, dotted and dashed curves coincide, so that planets migrate inward and gain mass from their surroundings. This is simply because the radiative feedback is switched on with a delay of half the initial period to allow the clump to contract sufficiently. There is then a bifurcation in trajectories of the planets once the feedback switches on. Planets with feedback (solid curves) accrete gas at smaller rates than their counterparts without feedback, as expected. Relatively low mass protoplanets, with $M_i = 0.5, 1$, and $2M_J$ migrate inward more rapidly than they contract independently of whether the feedback is on or off. However, for higher mass protoplanets, starting with $M_i = 4M_J$ (runs M4 and M4F), where the protoplanets end up in the Figure depend drastically on the feedback. The $M_i = 4M_J$ planet without feedback accretes mass very rapidly and becomes a brown-dwarf mass object with mass of $M_p = 35M_J$, having migrated to $a \approx 34$ AU. In contrast, the $M_i = 4M_J$ planet with feedback grows in mass much slower, reaching the maximum mass of only $8M_J$. At this point the planet is already at $a \approx 30$ AU, where tidal torques from the star start to

unbind it. Eventually the planet migrates to $a \sim 25$ AU and gets totally unbound.

Similarly, the $M_p = 8M_J$ with feedback grows to $M_p = 17M_J$; but, having migrated too closely in, gets unbound at $a \sim 20$ AU. The same case without feedback becomes as massive as $M_p \sim 60M_J$, at which point it collapses into the second configuration. This proto-“planet” migrates very little, ending up close to where it started at the end of the simulation, and actually evolving to $M_p \approx 130M_J$ (see §5).

Finally, the heaviest perturbation runs considered here, $M_i = 16M_J$, end up as sink particles, $M_p \approx 58M_J$ and $M_p \approx 70M_J$, for the feedback and no feedback runs, respectively. In both of these cases the sink continues to grow in mass. However, even in this case (M16F), the feedback has apparently played a role in the evolution of the protoplanet. The final separation of the sink particle from the parent star is smaller in run M16F than it is in M16.

To summarise, all of the runs presented here, with or without feedback, yielded one of the two possible outcomes: (a) an inward migration of lower mass clumps, followed by their tidal disruption at the inner disc, or (b) rapid accretion of gas onto the more massive protoplanets from the disc, followed by collapse to the second core (proto brown dwarf). We shall see later on that the sink particles introduced continue to grow rapidly. The end result of (b) is thus formation of a low mass secondary star in orbit around the primary. The role of radiative preheating from the protoplanet is to only shift the dividing mass of the planet at which the transition from evolutionary path (a) to that of (b) takes place.

5 CLUMP ACCRETION VERSUS MIGRATION

In this section we contrast the $M_i = 8M_J$ simulation without feedback (M8) with the same M_i run but with feedback (M8F). These particular simulations exemplify the effects of the radiative feedback from protoplanets on its surroundings in the most clear way.

The top panel in Figure 3 shows the time evolution of the protoplanetary mass, whereas the bottom panel of the figure shows the planet-star separation versus time. The solid and dotted curves correspond to simulations with feedback and without, respectively. The dotted curve has a discontinuity in it to emphasise the “phase transition” that occurs in the evolution of simulation M8. Before time $t \approx 2300$ yrs, the clump is molecular, e.g., it is the first core in the usual terminology (e.g., Larson 1969), whereas after that time molecular hydrogen in the clump dissociates, so that the clump collapses to much higher densities and becomes the second core. The latter phase of the evolution is shown with the red color. We cannot continue to resolve such high densities due to numerical limitations. A sink particle with sink radius of 5 AU is introduced at that point.

The sink continues to accrete gas from the disc. Note that its accretion rate is not steady. There is a particularly rapid accretion episode at $t \approx 3500$ yrs, when the secondary sink disrupts and then accretes a gas clump that migrated from the outer disc. The latter clump was not introduced in the disc artificially; instead it formed during the simulation due to the perturbations of the “original” protoplanet we inserted. More on this below in this section.

In contrast, in simulation M8F, the mass of the proto-

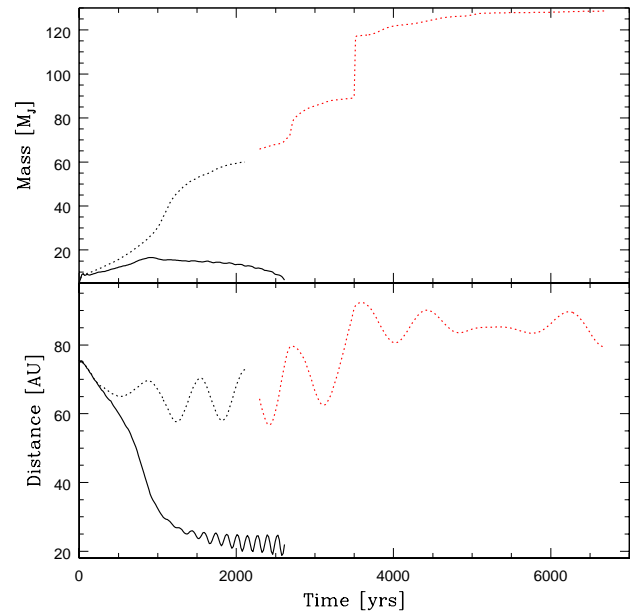


Figure 3. Time evolution of the protoplanet’s mass (top panel) and separation (bottom panel) for simulation M8 (dotted; no feedback) and M8F (solid; with protostellar feedback). In the simulation without feedback, the clump collapses into a second core, at which point we model it as a sink particle, and plot its evolution with the red color. This sink particle then continues to gain mass from the disc rapidly and grows to mass of almost $0.13 M_{\odot}$ by the end of the simulation.

planet varies by about a factor of two while it spirals in on the timescale of about 10^3 years. The simulation ends with the planet destroyed by tidal forces at $a \sim 20$ AU.

Figure 4 presents the same simulations but focuses on the interaction between the planet and the disc. In figure 4, left and right column panels correspond to simulations M8 and M8F, respectively. The top most panel in the figure show the gas column density at time $t = 2000$ yrs for the simulations. In both cases the gas clumps at the top right corner, and further gas concentrations on the way to contracting into clumps at $R \sim 130$ AU, are not the ones we are interested in. As explained in section 3.3, we avoided as much as possible formation of these additional clumps by using the initial condition with a marginally stable disc. We emphasise that no clumps develop in the control simulation that we used to initialise the disc (cf. section §3.3). Therefore, it is clear that these “uninteresting” clumps were spawned by gravitational disc instability *amplified* by the introduction of the clump that we do study here. We do not introduce feedback inside and around the second generation clumps as we are not interested in those.

The first generation clumps are located in the inner disc in both cases. In the case without feedback, the clump stalls close to its initial location, at $R \sim 75$ AU. In the simulation with feedback, on the other hand, the clump is at $R \sim 25$ AU at that time (these results are in accord with figure 3, of course).

The middle and the bottom row of panels in figure 4 show the total gas mass in radial annuli (for information, the bin size is proportional to radius R) in the simulation M8

and M8F (left and right, respectively). The protoplanet is identifiable as a strong maximum inside 100 AU; additional maxima outside this region are the secondary clumps that we do not study here.

The effects of the protoplanet in run M8F on its surrounding disc are barely discernable, whereas in the no-feedback case M8 the protoplanet strongly alters the disc structure. Namely, in the latter case the protoplanet almost succeeds in carving out a gap around its radial position. The deficit of gas near the planet's location in simulation M8 is visible in the top (left) panel of the figure, and is further quantified in the middle and the bottom left panels. There is a deep depression in the disc mass on both sides of the planet. It is clear that this protoplanet settles into the type II migration regime, and this must be the main reason why the planet's migration rate is much slower than that for the other simulation.

In the simulation with feedback, on the other hand, the protoplanet's mass stays low enough to not open the gap in the disc. Indeed, the panels in the right column of figure 4 show that there is not even a depression in the radial profile of the disc mass. As argued by Baruteau et al. (2011), when no gap is opened, protoplanets are expected to migrate inward very rapidly, i.e., nearly dynamically. In our simulation this situation persists until the planet arrives near the inner edge of the disc. Note that the planet's orbit is then not exactly circular and the eccentricity increases with time (cf. the bottom panel in figure 3).

The main driver of these differences in the planet-disc interaction is the mass of the protoplanet, whose evolution is strongly influenced by the radiative feedback (preheating) from the clump, as we now show.

6 THE ATMOSPHERE OF THE CLUMP

We now consider the behaviour of the material near the protoplanet in simulations M8 and M8F. As explained previously, these two cases differ significantly at late times, when both the radial position and the mass of the protoplanets diverge (e.g., see fig. 3). For a meaningful quantitative comparison we therefore contrast the clumps soon after the feedback is turned on, just as their evolution starts to take different paths, at time $t = 500$ years (cf. figure 3). Both the mass and the radial position of the clumps are approximately the same at that time.

Figure 5 shows temperature, density and radial velocity of gas particles as a function of distance, r , from the protoplanet's centre (defined as its densest point). Red and black dots and curves correspond to simulation M8F and M8, respectively. In the top panels dots show temperature (left) and density (right panel) at the location of individual SPH particles. The left top panel shows that the density in the atmosphere of the protoplanet without feedback is $\sim 2 - 3$ times higher than in simulation M8F.

The curves in the right panel of figure 5 show the radiative zero solution temperature, T_{rad} , defined by equation 3. Here $M_p(r)$ is the minimum of the enclosed mass within radius r and $8M_J$. These curves play no role in the actual simulation, but are presented here to make a comparison with the radiative zero solution.

There is a significant dispersion in SPH particles' tem-

perature at the same distance from the planet's centre, which is to be expected given that the geometry ceases to be quasi-spherical and becomes disc-like farther away from the planet. Nevertheless, it is clear that the gas around the planet at $r \sim 10$ AU is significantly colder than T_{rad} for the simulation without feedback (M8). At the same time, gas may be significantly hotter at the same location for simulation M8F, with the mean value of T following T_{rad} approximately.

The importance of this difference in the temperature profile near the planet is best appreciated in the bottom panel of figure 5, where we show the mean radial velocity (defined with respect to the planet's centre, of course) of SPH particles for the two simulations. The simulation without feedback (black curve) has a significant negative radial velocity, indicating infall, e.g., accretion. The maximum infall velocity is nearly 0.4 km s^{-1} at ~ 10 AU, which is slightly above the isothermal sound speed for molecular gas at temperature of 30 K, $c_s = 0.3 \text{ km s}^{-1}$ (cf. the black dots at this distance in the top right panel). This shows that gas is contracting quite rapidly onto the protoplanet in simulation M8, fuelling its rapid growth in mass.

In contrast, in simulation with radiative preheating (M8F, red curve), the maximum infall velocity, reached at ~ 15 AU, is a fraction of the gas sound speed, and becomes several times smaller than that closer in. Gas accretion is thus strongly hindered due to larger pressure gradient around the clump, which in itself is due to radiative preheating of the material near planet. This protoplanet is thus surrounded by a quasi-static atmosphere, as expected based on our approximate analytical theory.

These differences only get amplified at later times, as Figure 6 shows, where we show exactly same quantities but at time $t = 900$ yrs. The M8F clump actually starts to loose mass rather than gain it (cf. fig. 3), as is seen from a positive radial velocity in the bottom panel. This is in stark contrast to simulation M8 (no feedback), where the inward gas velocity reaches almost 1 km sec^{-1} .

7 DISCUSSION

In this paper we studied the evolution of a self-gravitating gas clump in a marginally gravitationally stable disc. We found that below a certain critical clump mass, M_{cr} , gas clumps migrate inward and get tidally disrupted quickly. Above this mass the clumps accrete gas from the disc rapidly, eventually becoming as massive as several tens of Jupiter masses. At such a high mass the gas clumps collapse into the second core configuration due to Hydrogen molecules dissociation (Larson 1969; Masunaga & Inutsuka 2000). These clumps become too massive for the disc to be transported inward rapidly. Therefore they stall and continue to grow by accretion, becoming massive brown dwarfs or low mass companions to the host star.

We also studied how this behaviour changes if the radiative output of the protoplanet due to its contraction luminosity is taken into account. We found that the qualitative behaviour of the simulations did not change, except the value of M_{cr} increases. In particular, in the simulations without radiative preheating from the planet, we obtained M_{cr} between 2 and 4 M_J , whereas with preheating M_{crit} rises to

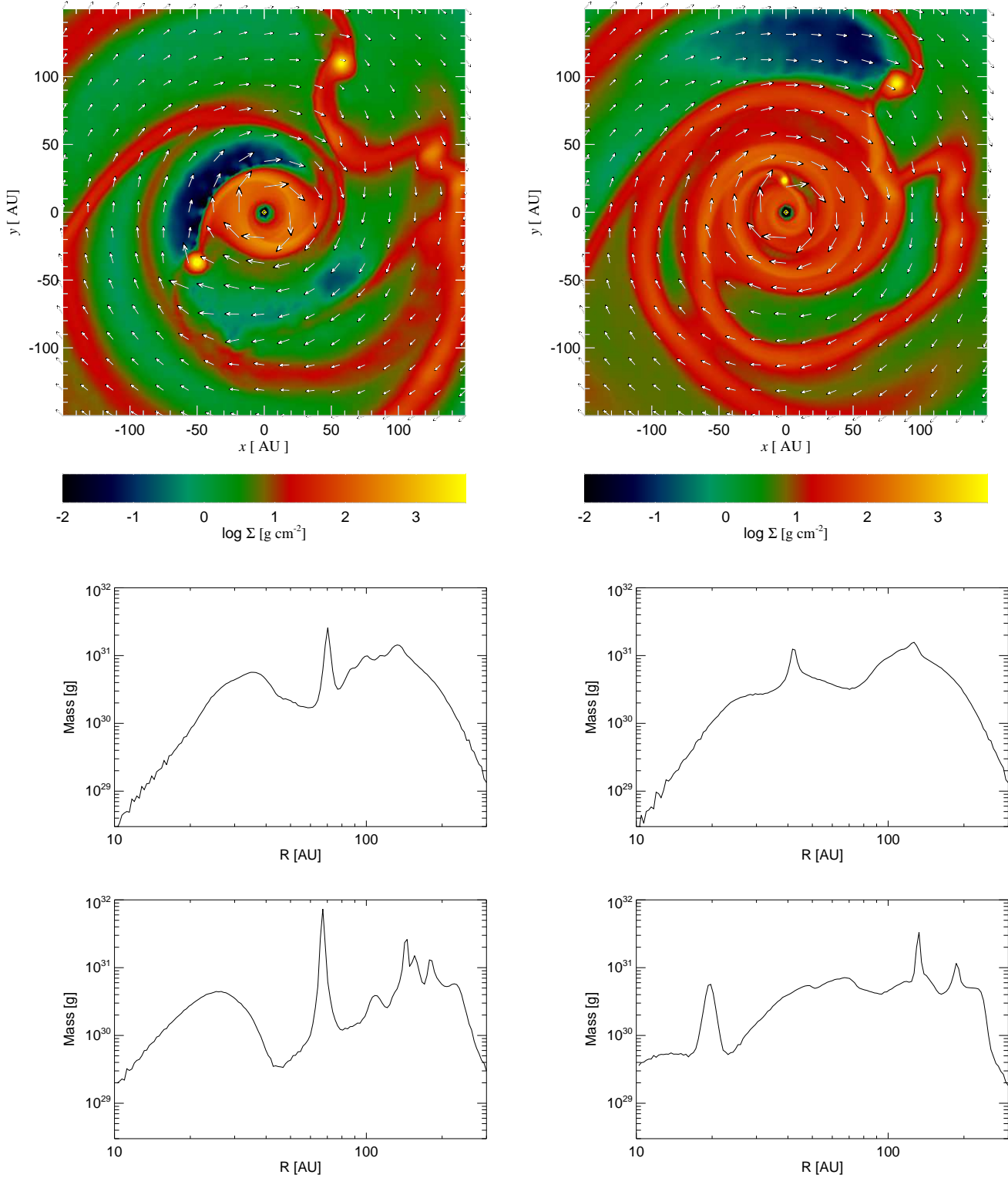


Figure 4. **Left column:** simulation M8 (no feedback), **Right:** simulation M8F, with feedback. The top row of panels show the disc surface density profiles at time $t = 2000$ yrs, whereas the row in the middle and on the bottom show gas mass in radial bins at time $t = 1200$ and 2100 yrs, respectively. See §5 for more detail.

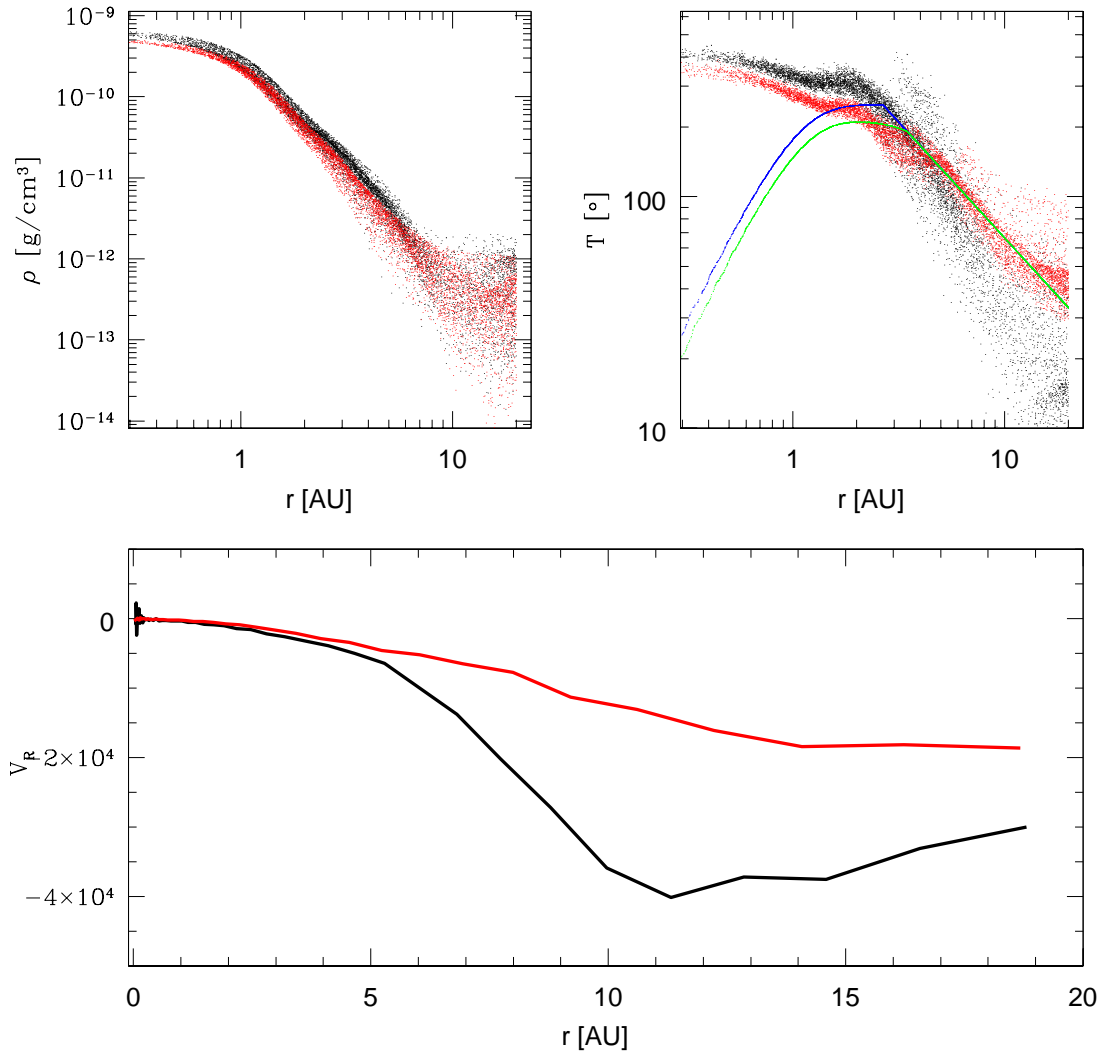


Figure 5. Internal structure of two clumps for a simulation M8F with radiative feedback (red color) and M8 (without feedback, black color) at time $t = 500$ yrs. Top left and top right panels show SPH particle temperature and density, respectively. The blue and the green curves show the radiative temperature T_{rad} from equation 9.

between $8M_J$ and $16M_J$. This result is consistent with the approximate analytical argument, presented in §2, similar in spirit to the well known Core Accretion result (Mizuno 1980; Stevenson 1982). This argument shows that radiative preheating from the clump may be sufficiently important to arrest gas accretion for clumps smaller than $\sim 6M_J$ (see equation 6). Having said this, we note that for clumps less massive than $\sim 2M_J$, inward migration appears so rapid that the outcome is similar whether the pre-heating is included or not: the clump is tidally disrupted at a few tens of AU.

The qualitative behaviour found in this paper – migration and tidal disruption of low mass clumps, but migration stalling and rapid gas accretion commencing for high mass clumps – is likely to be general for marginally stable discs. We are however certain that the critical mass M_{cr} itself is likely to depend on the disc opacity, mass, radial location

of where the gas clump is born, and the surrounding temperature of the disc. For example, higher disc temperatures may render radiative preheating from the clump ineffective in supporting the radiative atmosphere. A fuller investigation of the parameter space is planned in the near future.

Despite the fact that our study only covers a small fraction of the available parameter space, we believe that the sensitivity of the final fate of the clump to its initial mass (and other parameters in the problem, as discussed above), and such detail as radiative preheating of gas near the clump, is an important result to note. We believe this sensitivity may be the reason why different groups of numerical simulators obtain widely differing results, with some finding that massive self-gravitating discs around young stars mainly fragment onto brown dwarfs and low mass stars (Stamatellos & Whitworth 2008, 2009a), whereas others find that young gaseous clumps mainly migrate and get

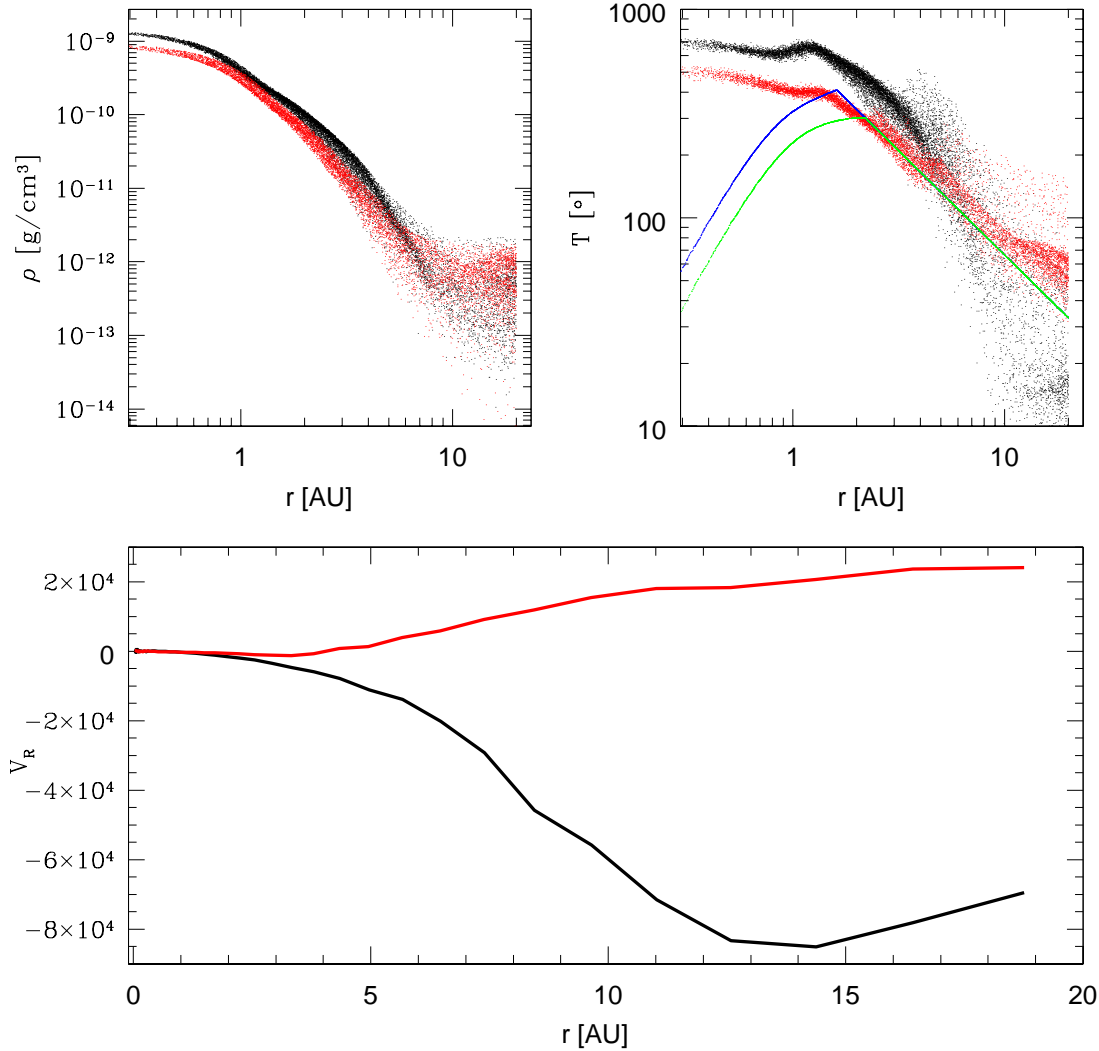


Figure 6. Same as figure 5 but at time $t = 900$ yrs. Note that the radiative preheating case M8F develops a positive radial velocity at that time (red curve in the bottom of the figure).

tidally disrupted (e.g., Boley et al. 2010; Cha & Nayakshin 2011), see also Zhu et al. (2012). In our opinion, it is possible that relatively small differences in the numerical techniques and/or regions of the parameter space studied may be sufficient to lead to divergent results obtained in those previous studies.

8 ACKNOWLEDGMENTS

Theoretical astrophysics research in Leicester is supported by an STFC Rolling Grant. This research used the ALICE High Performance Computing Facility at the University of Leicester, and the DiRAC Facility jointly funded by STFC and the Large Facilities Capital Fund of BIS.

REFERENCES

- Armitage P. J., 2010, *Astrophysics of Planet Formation*
 Baruteau C., Meru F., Paardekooper S.-J., 2011, *MNRAS*, 416, 1971
 Boley A. C., Hayfield T., Mayer L., Durisen R. H., 2010, *Icarus*, 207, 509
 Cha S.-H., Nayakshin S., 2011, *MNRAS*, 415, 3319
 Durisen R. H., Boss A. P., Mayer L., Nelson A. F., Quinn T., Rice W. K. M., 2007, *Protostars and Planets V*, 607–622
 Galvagni M., Hayfield T., Boley A. C., Mayer L., Roskar R., Saha P., 2012, *ArXiv e-prints*
 Gammie C. F., 2001, *ApJ*, 553, 174
 Helled R., Schubert G., 2008, *Icarus*, 198, 156
 Johnson B. M., Gammie C. F., 2003, *ApJ*, 597, 131
 Larson R. B., 1969, *MNRAS*, 145, 271
 Lodato G., Rice W. K. M., 2005, *MNRAS*, 358, 1489
 Machida M. N., Inutsuka S.-i., Matsumoto T., 2011, *ApJ*, 729, 42
 Masunaga H., Inutsuka S.-i., 2000, *ApJ*, 531, 350
 Mayer L., Quinn T., Wadsley J., Stadel J., 2004, *ApJ*, 609, 1045

- Meru F., Bate M. R., 2011, MNRAS, 410, 559
Michael S., Durisen R. H., Boley A. C., 2011, ApJL, 737, L42+
Mizuno H., 1980, Progress of Theoretical Physics, 64, 544
Nayakshin S., 2010a, MNRAS, 408, L36
Nayakshin S., 2010b, MNRAS, 408, 2381
Nayakshin S., 2011, MNRAS, 416, 2974
Rafikov R. R., 2005, ApJL, 621, L69
Rice W. K. M., Lodato G., Armitage P. J., 2005, MNRAS, 364,
L56
Shakura N. I., Sunyaev R. A., 1973, A&A, 24, 337
Stamatellos D., Whitworth A. P., 2008, A&A, 480, 879
Stamatellos D., Whitworth A. P., 2009a, MNRAS, 392, 413
Stamatellos D., Whitworth A. P., 2009b, MNRAS, 400, 1563
Stevenson D. J., 1982, P&SS, 30, 755
Vorobyov E. I., Basu S., 2006, ApJ, 650, 956
Vorobyov E. I., Basu S., 2010, ApJ, 719, 1896
Zhu Z., Hartmann L., Nelson R. P., Gammie C. F., 2012, ApJ,
746, 110